Analytical Methods

PAPER

View Article Online
View Journal | View Issue

Published on 22 January 2014. Downloaded by Michigan State University on 25/01/2016 00:09:49.

Cite this: *Anal. Methods*, 2014, **6**, 2080

Amplified inhibition of the electrochemical signal of graphene–thionine nanocomposites using silica nanoprobes for ultrasensitive electrochemical immunoassays

Guosong Lai,*[a] Cuiying Yin,[a] Xiangen Tan,[a] Haili Zhang[a] and Aimin Yu[ab]

Received 4th January 2014
Accepted 22nd January 2014

DOI: 10.1039/c4ay00020j

www.rsc.org/methods

An ultrasensitive immunoassay method was developed based on the amplified inhibition of the electrochemical signal of graphene–thionine nanocomposites. The graphene–thionine nanocomposite was prepared by one-step reduction of graphene oxide in thionine solution and used to modify a glassy carbon electrode. The immunosensor was prepared by stepwise assembly of gold nanoparticles (Au NPs) and a capture antibody at this nanocomposite modified electrode. The thionine on the immunosensor surface exhibited a good electrochemical signal which was further promoted by the presence of Au NPs. After a sandwich immunoreaction, the current response of the immunosensor decreased due to the formation of a dielectric antibody–antigen immunocomplex on its surface. This current decrease could be further amplified by the captured antibody conjugated silica nanosphere with low electric conductivity. Based on this amplified signal inhibition mechanism, a novel detection strategy for the ultrasensitive electrochemical immunoassay was developed. Using human IgG as a model protein, a wide linear range in four orders of magnitude and a low detection limit down to 7 pg mL^{-1} were achieved. In addition, the immunosensor has low cost, satisfactory reproducibility and stability, and acceptable reliability, thus providing promising potential for clinical applications.

1. Introduction

Recently, electrochemical immunosensors have shown great success in the accurate determination of protein biomarkers due to their unique advantages including high selectivity, low cost and good portability.[1–3] Typically, various enzyme labels are required to be used in these methods in order to produce the corresponding electrochemical signal for the sandwich immunoassays and achieve sensitive analyte measurements. However, the relatively high cost and low storage stability of the enzyme biomolecules may limit their wide applications.[4] Moreover, the electron transfer resistance caused by the dielectric antibody–antigen immunocomplex formed on the immunosensing surface can weaken their electrochemical signal response to some degree, which may further hinder the improvement in analytical performance to achieve a lower detection limit and a wider linear range.

Except for the enzyme, some electroactive indicators such as thionine (TH),[5,6] ferrocene[7,8] and methylene blue[9,10] can be also used for the signal tracing in the electrochemical bioassay field. As the impedance effect of the antibody–antigen immunocomplex can induce an obvious signal decrease of these electrochemical indicators modified on the electrode surface, many direct immunoreaction-based label-free electrochemical immunoassay methods have been easily developed in recent years.[5,11–14] Meanwhile, owing to their excellent electron transfer ability, various nanomaterials are commonly used to hybridize with these indicators for promoting their signal responses and achieving higher sensitivity.

As the latest nanomaterial star, graphene has recently gained increasing interest in a great variety of research fields due to its excellent physical and chemical properties.[15,16] Because graphene is hydrophobic and can not be dispersed in most solvents while hydrophilic graphene oxide (GO) has bad conductivity, chemical reduction of graphene oxide along with proper surface functionalization is commonly adopted to produce reduced graphene oxide (rGO) with desired properties and application potential for electrochemical biosensing.[17–19] Compared with the covalent and assembly methods, the π-rich surface domains of graphene enable it to be easily conjugated with the electrochemical indicator of TH with a water-soluble planar aromatic structure *via* the non-covalent π–π stacking interaction and thus obtain a useful electroactive nanocomposite.[20,21] In the previous reports, GO was often reduced first by hydrazine[20] or

[a]*Hubei Collaborative Innovation Center for Rare Metal Chemistry, Hubei Key Laboratory of Pollutant Analysis & Reuse Technology, Department of Chemistry, Hubei Normal University, Huangshi 435002, P.R. China. E-mail: laiguosong@hotmail.com; Fax: +86-714-6573832; Tel: +86-714-6515602*

[b]*Faculty of Science, Engineering and Technology, Swinburne University of Technology, Hawthorn, VIC 3122, Australia*

This journal is © The Royal Society of Chemistry 2014

Published on 22 January 2014. Downloaded by Michigan State University on 25/01/2016 00:09:49.

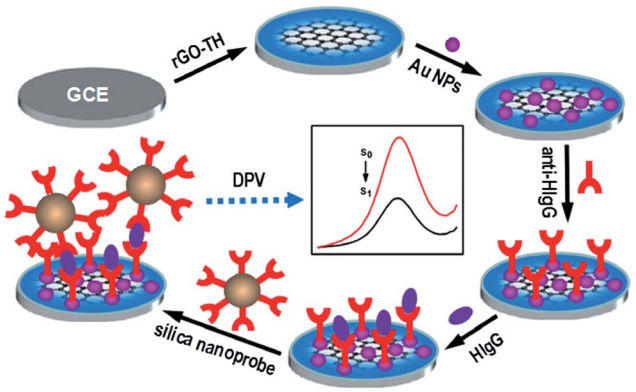

Scheme 1 Schematic representation of the preparation process of the immunosensor and the electrochemical detection strategy based on the sandwich immunoassay.

ascorbic acid[21] and then conjugated with TH. In fact, the good reducing property of thionine indicates that it may also serve as the reducing agent of GO. Herein, we tried the one-step reduction of GO in a thionine solution and achieved the easy preparation of rGO–TH nanocomposites in this work. Based on the electrode modification with the as-prepared rGO–TH and stepwise assembly of gold nanoparticles (Au NPs) and capture antibodies on its surface, an immunosensor was successfully constructed for the electrochemical immunoassay (Scheme 1).

In addition, it is worthwhile to note that the conventional label-free immunoassays often have limited sensitivity which makes them difficult to carry out the accurate measurement of low-abundant protein biomarkers in real serum samples. Therefore, the development of some strategies to amplify the electrochemical impedance for promoting the signal decrease induced by the direct immunoreaction should be an effective approach to achieve highly sensitive immunoassays. As a versatile nanomaterial, monodispersible silica nanospheres have shown wide applications in the biomedical and biosensing fields.[22–24] Considering their low semiconducting conductivity in the obstruction of the electron transfer on the electrode surface,[25–27] this work used the antibody functionalized silica nanoprobe to promote the sensitivity improvement of the rGO–TH nanocomposite based electrochemical immunosensor successfully. After a sandwich immunoreaction, the current response of rGO–TH in the immunosensor decreased due to the formation of a dielectric antibody–antigen immunocomplex on its surface. This current decrease was further amplified using the captured antibody conjugated silica nanospheres owing to their unique electrochemical impedance effect. Based on this amplified signal inhibition strategy, a novel ultrasensitive electrochemical immunoassay method was thus developed.

2. Experimental section

2.1. Reagent and materials

Human IgG (HIgG), mouse IgG (MIgG), and polyclonal rabbit anti-human IgG (anti-HIgG) were purchased from Wuhan Boster Biological Technology Ltd. Bovine serum albumin (BSA), human serum albumin (HSA) and (3-aminopropyl)-triethoxysilane were obtained from Sigma-Aldrich Chemical Co. (St. Louis, MO). Glutaraldehyde (25% aqueous solution) was purchased from Alfa Aesar China Ltd. Chloroauric acid ($HAuCl_4 \cdot 4H_2O$), tetraethoxysilane and TH were obtained from Shanghai Reagent Company (Shanghai, China). The bovine serum sample was obtained from Beijing Solarbio Science & Technology Ltd. Ultrapure water obtained from a Millipore water purification system (Milli-Q) was used in all assays. All other reagents were of analytical grade and used as received.

Phosphate-buffered solution (PBS) of pH 7.0 was prepared by mixing the stock solutions of 50 mM NaH_2PO_4 and Na_2HPO_4 and used as the working solution. A 50 mM pH 7.0 PBS containing 0.05% (w/v) Tween-20 (PBST) was used as the washing buffer and a 50 mM pH 7.0 PBS containing 3% (w/v) BSA was used as the blocking solution.

2.2. Apparatus

The electrochemical impedance spectra were recorded on a CHI 660 electrochemical workstation (CH Instruments, USA) in 5.0 mM $K_3Fe(CN)_6/K_4Fe(CN)_3$ (1 : 1) containing 0.10 M KCl. All other electrochemical experiments were performed on a CHI 830B electrochemical workstation (Chenhua, China). A conventional three-electrode system containing a platinum wire as the auxiliary electrode, a saturated calomel electrode as the reference electrode and a modified glassy carbon electrode (GCE, 3 mm diameter) as the working electrode was used throughout the electrochemical experiments. The FT-IR and UV-vis spectra were recorded using a Thermo Scientific Nicolet iD5 spectrometer (USA) and a Hitachi UV-3100 spectrometer (Japan), respectively.

2.3. Preparation of the immunosensor

The rGO–TH nanocomposite was first prepared by a one-step reduction method. Briefly, 2.0 mg GO was added to 10 mL of 2.0 mM TH solution and ultrasonicated for 30 min to obtain a homogenous dispersion. Then, this dispersion was heated to 100 °C and reacted overnight under continuous stirring. After thrice centrifugation and washing with water, the resulting rGO–TH nanocomposite was collected and dispersed in water at a concentration of 0.5 mg mL^{-1} for further use.

The preparation process of the immunosensor is illustrated in Scheme 1. Before modification, a GCE was polished with alumina slurries of 0.3 and 0.05 μm successively followed by rinsing thoroughly with ultrapure water until a mirror-like surface was obtained. After washing by ultrasonication in absolute ethanol and water and then drying at room temperature, 3 μL as-prepared rGO–TH nanocomposites were dropped onto the surface of the GCE and dried slowly in air. Subsequently, 10 μL of 13 nm colloidal Au NPs prepared by the conventional citrate reduction method[4] were cast onto the electrode surface for 8 h assembly. After washing with water to remove the loosely adsorbed Au NPs, 3 μL of 0.5 mg mL^{-1} anti-HIgG was applied to the GCE surface and incubated in a 100% moisture saturated environment overnight at 4 °C. The resulting electrode was washed three times with PBST and PBS to

Published on 22 January 2014. Downloaded by Michigan State University on 25/01/2016 00:09:49.

remove the loosely adsorbed antibody and then incubated with the blocking solution for 60 min at room temperature to block the possible remaining active sites against nonspecific adsorption. After washing again with PBST and PBS, the resulting immunosensor was finally obtained and stored at 4 °C in a dry environment prior to use.

2.4. Preparation of silica nanoprobes

Firstly, the monodispersible silica nanospheres with an average diameter of about 100 nm were prepared and amino-functionalized followed by the surface-activation with glutaraldehyde according to our previous reports.[24] After centrifugation and repeated washing with PBS, 2.0 mg of the aldehydized silica nanospheres were redispersed in 1.0 mL PBS containing 15 μg of anti-HIgG and reacted for 2 h at room temperature by gentle mixing. After centrifugation, the obtained bioconjugates were blocked with 3% BSA for 60 min, and then washed thrice with PBS and resuspended in 1.0 mL PBS containing 0.1% BSA as the nanoprobe dispersion.

2.5. Analytical procedure

Based on the sandwich-type immunoassay, the immunosensor was first incubated with a 15 μL drop of the HIgG standard solution or serum sample for 50 min at room temperature, followed by washing with PBST and PBS. Then, 15 μL of the silica nanoprobe dispersion was cast onto the immunosensor surface for another 50 min of incubation. After washing with PBST and PBS again, differential pulse voltammetry (DPV) at a step potential of 4 mV, a pulse amplitude of 50 mV and a pulse period of 0.2 s was performed in pH 7.0 PBS to record the current response for the quantitative analysis.

3. Results and discussion

3.1. Preparation and characterization of the rGO–TH nanocomposite

In this work, the rGO–TH nanocomposite was one-step prepared by using TH as both the reducing and stabilizing agent. Firstly, the as-prepared rGO–TH was characterized by FT-IR spectroscopy (Fig. 1A). Similar to the previous reports,[28,29] GO exhibited a strong C=O stretching vibration at 1735 cm^{-1}, a strong C=C stretching, skeletal vibrations from unoxidized graphitic domains at 1622 cm^{-1}, a broad absorption band at 3000–3500 cm^{-1} from O–H stretching vibration as well as a weak O–H deformation peak at 1400 cm^{-1}, a C–OH stretching peak at 1220 cm^{-1} and a C–O stretching peak at 1050 cm^{-1}. After reduction of GO by TH, the oxygen-containing functionalities of GO such as the C=O and C–O stretching vibration peaks almost disappeared completely while new strong absorption bands at 1600–1302 cm^{-1} from the skeletal vibrations of the phenyl ring of TH[30,31] were clearly observed in the IR spectrum of the formed nanocomposite. These results indicate that GO was successfully reduced by TH; meanwhile, TH was also conjugated with graphene through the π–π stacking interaction to form an rGO–TH nanocomposite. In addition, from the UV-vis spectrum of rGO–TH shown in Fig. 1B we can also find two obvious absorption peaks of TH at 280 nm and 598 nm.[5] This phenomenon further confirmed the successful preparation of the rGO–TH nanocomposite.

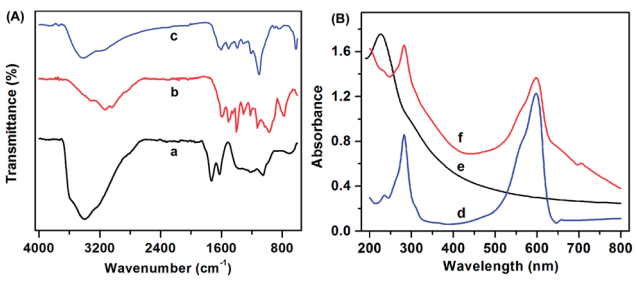

Fig. 1 (A) FT-IR and UV-vis spectra of GO (a and e), rGO–TH nanocomposites (b and f) and TH (c and d).

3.2. Preparation of the immunosensor

The as-prepared rGO–TH nanocomposite was then used to modify the electrode for the further assembly of Au NPs and the antibody on its surface to form an immunosensor. This step-by-step preparation process was characterized by monitoring the electrochemical behavior of TH modified on the electrode surface. From Fig. 2A we can find that the rGO–TH modified electrode showed a pair of well-defined redox peaks at the potentials of −0.080 V and −0.148 V (curve a), which is due to the excellent electrochemical behavior of TH conjugated with rGO. After Au NPs were further assembled on the electrode surface, its peak currents increased obviously (curve b). This phenomenon should be attributed to the excellent electron transfer acceleration from Au NPs introduced onto the electrode surface. The Au NP assembly also provided an ideal interface for the antibody immobilization through the specific interaction between noble-metal nanoparticles and protein biomolecules.[24] After immobilizing anti-HIgG on the electrode surface and further blocking the possible remaining active sites by BSA, however, the current response of the modified electrode showed an obvious decrease (curve c). This phenomenon should be attributed to the dielectric protein biomolecules attached to the electrode surface, which also indicates the successful preparation of the immunosensor.

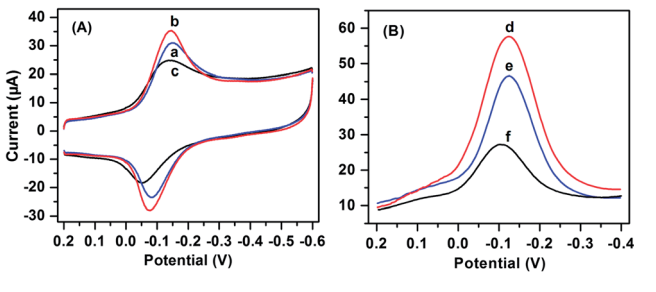

Fig. 2 (A) Cyclic voltammograms recorded at the rGO–TH (a), rGO–TH/Au NP (b) modified GCE and the immunosensor (c); (B) DPV responses of the immunosensor before (d) and after immunoreaction with 100 ng mL^{-1} HIgG based on the direct (e) and sandwich (f) immunoassay format.

This journal is © The Royal Society of Chemistry 2014

Published on 22 January 2014. Downloaded by Michigan State University on 25/01/2016 00:09:49.

3.3. Electrochemical immunoassay in the immunosensor

As a sensitive electroanalytical method, DPV was used to study the electrochemical response of the immunosensor towards the HIgG analyte. As shown in Fig. 2B, the immunosensor showed a sensitive DPV peak at the potential of −0.118 V (curve d). Compared with the current response before the immunoreaction, an obvious drop in the peak current of the immunosensor was observed after incubation with 100 ng mL^{-1} HIgG (curve e). This is due to the formation of a dielectric antibody–antigen immunocomplex on the electrode surface which further hinders the electrochemical signal of the rGO–TH nanocomposite. Further experiments showed that in comparison with this direct antigen–antibody immunoreaction in the immunosensor, when the antibody conjugated silica nanoprobe was further used for the sandwich immunoreaction, a drastic current decrease occurred in the immunosensor (curve f). This result suggests that the silica nanoprobe could greatly increase the electrochemical impedance of the immunosensor resulting in the amplified signal inhibition to the electrochemical indicator of TH.

In addition, electrochemical impedance spectroscopy was also used to characterize the interfacial resistance change during the immunosensor preparation and immunoassay process. As shown in Fig. 3, compared with the bare GCE, we can clearly find the obvious Nyquist diameter decrease after the electrode modification with the rGO–TH nanocomposite and the subsequent assembly of Au NPs on its surface. The results confirmed that both the rGO–TH and Au NPs modified on the electrode surface could greatly promote the electron transfer due to their excellent electrical conductivity and large specific surface area. However, the electrochemical resistance increased drastically after antibody immobilization and BSA blocking to obtain the immunosensor. This phenomenon further demonstrated that the immobilization of dielectric protein biomolecules could inhibit the electron transfer on the electrode surface. After incubation of 100 ng mL^{-1} HIgG in the immunosensor, an obvious resistance increase due to the formation of a dielectric antibody–antigen immunocomplex was also observed. Moreover, the Nyquist diameter resistance increased dramatically when the as-prepared silica nanoprobe was further used for the sandwich immunoreaction. These phenomena confirmed that the silica nanoprobe with an excellent impedance effect could greatly promote the electrochemical signal inhibition of the immunosensor. Hence, by combination of this amplified signal inhibition strategy and the sensitive electrochemical response of the rGO–TH based immunosensor, a novel ultrasensitive immunoassay method was thus developed.

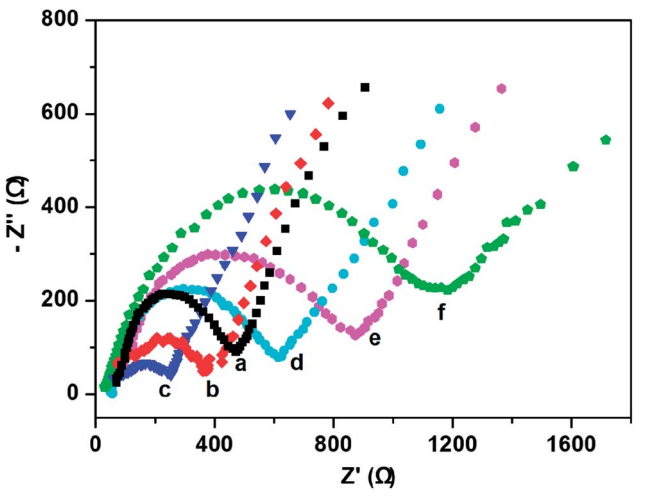

Fig. 3 Nyquist plots recorded at the bare GCE (a), rGO–TH (b) and rGO–TH/Au NP (c) modified GCE; and the immunosensor before (d) and after immunoreaction with 100 ng mL^{-1} HIgG based on the direct (e) and sandwich (f) immunoassay format.

3.4. Optimization of incubation time

To achieve excellent analytical performance of this method, the effect of incubation time on the DPV response of the immunosensor towards 10 ng mL^{-1} HIgG was investigated (Fig. 4). At room temperature, the DPV current response decreased with increasing incubation time used in the sandwich immunoassay and then tended to a constant value after 50 min, indicating the saturated binding of the sandwich immunoreaction on the electrode surface. Therefore, an incubation time of 50 min was selected for the sandwich immunoassay at room temperature.

3.5. Analytical performance

Based on the sandwich immunoassay, the electrochemical responses of the immunosensor towards different concentrations of HIgG were examined. From Fig. 5 we can observe that the DPV responses of the immunosensor decreased with the increasing concentrations of the analyte. The calibration curve showed a good linear relationship between the peak currents and the logarithm values of HIgG concentrations in the range from 0.01 to 100 ng mL^{-1} with a correlation coefficient of 0.9984. The detection limit at a signal-to-noise ratio of 3 was estimated to be 7 pg mL^{-1}. As shown in Table 1, this method showed excellent analytical performance with a wider linear range and a lower detection limit not only than many label-free electrochemical immunoassays[32–34] but also than some signal

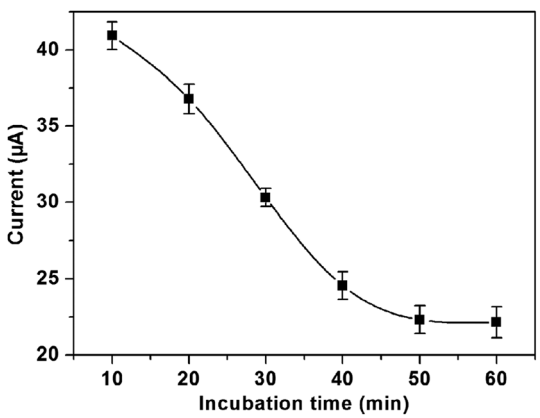

Fig. 4 Effect of incubation time on the DPV response of the immunosensor towards 10 ng mL^{-1} HIgG.

Published on 22 January 2014. Downloaded by Michigan State University on 25/01/2016 00:09:49.

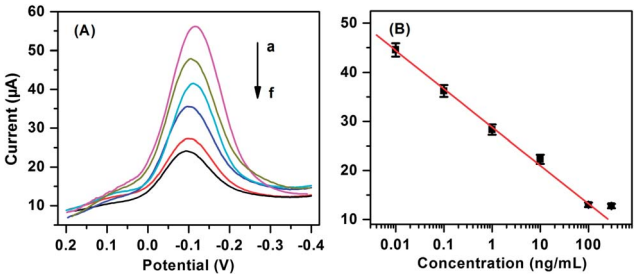

Fig. 5 DPV responses of the immunosensor towards different concentrations of HIgG using the proposed amplified signal inhibition strategy (A) and the calibration curve (B). Curves (a–f) correspond to HIgG at concentrations from 0.01 ng mL^{-1} to 300 ng mL^{-1}.

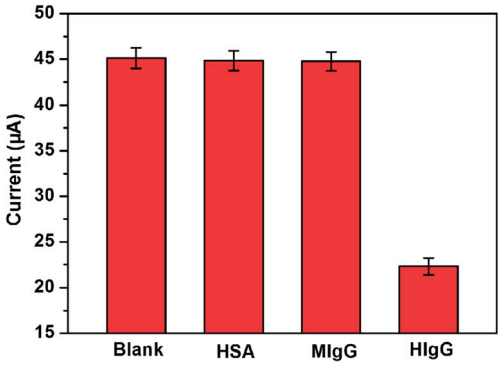

Fig. 6 DPV responses of the immunosensor towards the blank control, 1% HAS, 10 ng mL^{-1} MIgG and 10 ng mL^{-1} HIgG.

amplification strategy based electrochemical immunoassays[1,35–37] reported previously, which is very important for its practical applications.

3.6. Specificity, reproducibility, stability and reliability

MIgG and HSA were used to investigate the specificity of the immunosensor towards noncognate proteins. As shown in Fig. 6, no obvious current decrease over the blank control was observed when MIgG and HSA were used for the sandwich immunoassay in the immunosensor. However, this immunosensor showed an obvious current decrease towards the target protein of HIgG. These results indicate that the cross-reactivity of the immunosensor towards noncognate proteins was negligible.

In addition, five immunosensors were prepared for the repeated measurements of two different concentrations of HIgG. The coefficients of variation were 3.4% and 4.1% for 0.1 and 10 ng mL^{-1} HIgG, respectively. In addition, the immunosensor could retain 92% of the initial response for 10 ng mL^{-1} HIgG after a storage period of two weeks in dry air at 4 °C. These results indicate that the immunosensor had satisfactory reproducibility and stability.

In order to assess the possibility of this method for practical applications, different amounts of HIgG were added into bovine serum for recovery tests. The test results from three repeated experiments are listed in Table 2. The recoveries of the standard addition experiments were between 97% and 109% with the relative standard deviation (RSD) lower than 5.8%. These results

Table 2 Recovery tests of HIgG in bovine serum samples

No.	Added (ng mL^{-1})	Found (ng mL^{-1})	RSD (%)	Recovery (%)
1	0.1	0.097	5.8	97
2	1	1.03	5.3	103
3	10	10.9	4.7	109

Table 1 Comparison of the analytical performance of this method with those of some other electrochemical immunosensors for HIgG measurement[a]

Immunosensor	Detection strategy	Linear range	Detection limit	Ref.
GCE/rGO/CNT/anti-HIgG	Enzymatic catalysis by HRP labels	1–500 ng mL^{-1}	0.2 ng mL^{-1}	1
Gold electrode/cysteine/Au NP/anti-HIgG	Dopamine oxidation current inhibition based label-free immunoassay	0.82–90 ng mL^{-1}	0.25 ng mL^{-1}	32
Gold electrode/PTH–methylene blue/Au NP/anti-HIgG	$K_3Fe(CN)_6$ signal inhibition based label-free immunoassay	10–10 000 ng mL^{-1}	3 ng mL^{-1}	33
Gold electrode/protein A	Label-free electrochemical impedance spectroscopy	10–1000 ng mL^{-1}	5 ng mL^{-1}	34
SPCE/rGO–Au NP/anti-HIgG	Electrocatalytic reduction of oxygen by CNT/Pd NP labels	0.05–10 ng mL^{-1}	44 pg mL^{-1}	35
GCE/ferrocene–chitosan–ionic liquid/Au NP/anti-HIgG	Enzymatic catalysis by rGO-Au NP-HRP labels	0.2–500 ng mL^{-1}	50 pg mL^{-1}	36
Gold electrode/CNT–Fe_3O_4/anti-HIgG	Enzymatic catalysis by HRP labels	30–1000 ng mL^{-1}	25 ng mL^{-1}	37
GCE/rGO–TH/Au NP/anti-HIgG	Amplified signal inhibition by silica nanoprobes	0.01–100 ng mL^{-1}	7 pg mL^{-1}	This work

[a] CNTs: carbon nanotubes; HRP: horseradish peroxidase; PTH: polythionine; SPCE: screen-printed carbon electrode.

 This journal is © The Royal Society of Chemistry 2014

Published on 22 January 2014. Downloaded by Michigan State University on 25/01/2016 00:09:49.

indicate the acceptable reliability of the proposed method for real sample analysis.

4. Conclusions

A novel ultrasensitive immunoassay method was developed based on the amplified inhibition of the electrochemical signal of rGO–TH nanocomposites using silica nanoprobes. The one-step reduction of GO in TH solution provided a simple method to prepared the well-dispersed rGO–TH nanocomposite which was successfully used as an ideal material for the electrode modification and as an excellent electrochemical indicator for immunoassays. After sandwich immunoreaction, the electrochemical signal of the rGO–TH decreased owing to the impedance effect of the dielectric antibody–antigen immunocomplex formed on the immunosensor surface. This current decrease could be further amplified using the captured silica nanoprobes which enabled the development of a novel ultrasensitive immunoassay method. This method showed excellent analytical performance for the protein analyte determination with a wide linear range and low detection limit. In addition, the immunosensor had low cost, good reproducibility and stability, and satisfactory reliability. Thus, this method provides promising potential for practical applications.

Acknowledgements

The authors gratefully acknowledge the financial support from the National Natural Science Foundation of China (21205031), Science and Technology Foundation for the Creative Research Group of HBDE (T201311) and ANZ Trustees Medical Research & Technology in the Victoria program (CT20692).

References

1 Y. Liu, Y. Liu, H. B. Feng, Y. M. Wu, L. Joshic, X. Q. Zeng and J. H. Li, *Biosens. Bioelectron.*, 2012, **35**, 63–68.
2 Z. Z. Yin, Y. Liu, L. P. Jiang and J. J. Zhu, *Biosens. Bioelectron.*, 2011, **26**, 1890–1894.
3 F. Yang, Y. Q. Chai, R. Yuan, J. Han, Y. L. Yuan, N. Liao and Z. H. Yang, *Anal. Methods*, 2013, **5**, 5279–5285.
4 G. S. Lai, L. L. Wang, J. Wu, H. X. Ju and F. Yan, *Anal. Chim. Acta*, 2012, **721**, 1–6.
5 Q. Wei, K. X. Mao, D. Wu, Y. X. Dai, J. Yang, B. Du, M. H. Yang and H. Li, *Sens. Actuators, B*, 2010, **149**, 314–318.
6 J. Tang, D. P. Tang, R. Niessner, D. Knopp and G. N. Chen, *Anal. Chim. Acta*, 2012, **720**, 1–8.
7 T. Li and M. H. Yang, *Sens. Actuators, B*, 2011, **158**, 361–365.
8 Y. Y. Ding, D. Li, B. Li, K. Zhao, W. Du, J. Y. Zheng and M. H. Yang, *Biosens. Bioelectron.*, 2013, **48**, 281–286.
9 F. Y. Kong, X. Zhu, M. T. Xu, J. J. Xu and H. Y. Chen, *Electrochim. Acta*, 2011, **56**, 9386–9390.
10 S. Khezrian, A. Salimi, H. Teymourian and R. Hallaj, *Biosens. Bioelectron.*, 2013, **43**, 218–225.
11 J. D. Qiu, R. P. Liang, R. Wang, L. X. Fan, Y. W. Chen and X. H. Xia, *Biosens. Bioelectron.*, 2009, **25**, 852–857.
12 X. Q. Ran, R. Yuan, Y. Q. Chai, C. L. Hong and X. Q. Qian, *Colloids Surf., B*, 2010, **79**, 421–426.
13 X. M. Huang, X. Deng and D. Wu, *Anal. Methods*, 2012, **4**, 3575–3579.
14 X. B. Sun and Z. F. Ma, *Anal. Chim. Acta*, 2013, **780**, 95–100.
15 D. A. C. Brownson, D. K. Kampouris and C. E. Banks, *Chem. Soc. Rev.*, 2012, **41**, 6944–6976.
16 X. D. Xue, D. Wei, R. Feng, H. Wang, Q. Wei and B. Du, *Anal. Methods*, 2013, **5**, 4159–4164.
17 Y. X. Xu and G. Q. Shi, *J. Mater. Chem.*, 2011, **21**, 3311–3323.
18 S. Bai and X. P. Shen, *RSC Adv.*, 2012, **2**, 64–98.
19 S. Liu, J. Q. Tian, L. Wang, Y. L. Luo, W. B. Lu and X. P. Sun, *Biosens. Bioelectron.*, 2011, **26**, 4491–4496.
20 L. M. Zhu, L. Q. Luo and Z. X. Wang, *Biosens. Bioelectron.*, 2012, **35**, 507–511.
21 F. Y. Kong, M. T. Xu, J. J. Xu and H. Y. Chen, *Talanta*, 2011, **85**, 2620–2625.
22 K. Payton, S. Santra and P. Tallury, *Nanomedicine*, 2008, **3**, 579–592.
23 J. L. Vivero-Escoto, R. C. Huxford-Phillips and W. B. Lin, *Chem. Soc. Rev.*, 2012, **41**, 2673–2685.
24 G. S. Lai, J. Wu, C. Leng, H. X. Ju and F. Yan, *Biosens. Bioelectron.*, 2011, **26**, 3782–3787.
25 D. P. Tang, R. Yuan, Y. Q. Chai and Y. Z. Fu, *Electrochem. Commun.*, 2005, **7**, 177–182.
26 T. I. Yang, R. N. C. Brown, L. C. Kempel and P. Kofinas, *Nanotechnology*, 2011, **22**, 105601.
27 Y. Zhuo, R. Yuan, Y. Q. Chai and C. L. Hong, *Analyst*, 2010, **135**, 2036–2042.
28 Y. X. Xu, H. Bai, G. W. Lu, C. Li and G. Q. Shi, *J. Am. Chem. Soc.*, 2008, **130**, 5856–5857.
29 M. J. Fernández-Merino, L. Guardia, J. I. Paredes, S. Villar-Rodil, P. Solís-Fernández, A. Martínez-Alonso and J. M. D. Tascón, *J. Phys. Chem. C*, 2010, **114**, 6426–6432.
30 Y. H. Ding, Z. Q. Chen, J. Xie and R. Guo, *J. Colloid Interface Sci.*, 2008, **327**, 243–250.
31 Z. Li, Y. Huang, L. Chen, X. L. Qin, Z. Huang, Y. P. Zhou, Y. Meng, J. Li, S. Y. Huang, Y. Liu, W. Wang, Q. J. Xie and S. Z. Yao, *Sens. Actuators, B*, 2013, **181**, 280–287.
32 L. Y. Zhang, Y. Liu and T. Chen, *Int. J. Biol. Macromol.*, 2008, **43**, 165–169.
33 L. P. Qiu, C. C. Wang, P. Hu, Z. S. Wu, G. L. Shen and R. Q. Yu, *Talanta*, 2010, **83**, 42–47.
34 H. L. Qi, C. Wang and N. Cheng, *Microchim. Acta*, 2010, **170**, 33–38.
35 C. Leng, J. Wu, Q. N. Xu, G. S. Lai, H. X. Ju and F. Yan, *Biosens. Bioelectron.*, 2011, **27**, 71–76.
36 Y. C. Yang, S. W. Dong, T. Shen, C. X. Jian, H. J. Chang, Y. Li and J. X. Zhou, *Electrochim. Acta*, 2011, **56**, 6021–6025.
37 H. Zarei, H. Ghourchian, K. Eskandari and M. Zeinali, *Anal. Biochem.*, 2012, **421**, 446–453.